Int. J. Solids Structures Vol. 18, No. 5, pp. 397–410, 1982
Printed in Great Britain.

0020-7683/82/050397-14$03.00/0
Pergamon Press Ltd.

HARMONIC WAVES IN A PERIODICALLY LAMINATED MEDIUM

A. H. SHAH
Department of Civil Engineering, University of Manitoba, Winnipeg, Canada

and

S. K. DATTA
Department of Mechanical Engineering, University of Colorado, Boulder, CO 80309, U.S.A.

(*Recieved* 10 *May* 1981; *in revised form* 20 *October* 1981)

Abstract—A stiffness method using the continuity of displacement and traction at the interfaces of a periodically laminated composite medium and the Floquet's Theory has been presented here for studying harmonic wave propagation in a layered composite. Both plane strain and antiplane strain problems have been studied. The equations have been developed for both isotropic and anisotropic layers. Numerical results are presented for the dispersion spectrum for propagation in a periodic two-layered medium and these are shown to compare well with available exact results. Finally, numerical results are presented for a boron–aluminum composite medium, which is modelled as a composition of anisotropic and isotropic layers.

INTRODUCTION

The increasing use of fiber-reinforced composites in structural applications has generated extensive research efforts in the area of dynamic behavior of periodically laminated medium. Various approximate theories have been proposed. Some of these are the effective modulus theory[1, 2], effective stiffness theory[3, 4], mixture theory[5–7] and the theory of interacting continuum[8, 9]. Recently in [10] higher order plate theory together with a smoothing operation has been used to study the dispersion characteristics of two-layer periodic laminated media.

In addition to the approximate analysis mentioned above exact solutions for wave propagation in laminated media have been presented. The antiplane[11–13] and plane strain[14] problems have been dealt with by imposing the displacement and stress continuity conditions at the interfaces. Recently[15–17] the dispersion characteristics for harmonic wave propagation have been analyzed by using Floquet's theory in conjunction with the elasticity solutions.

In all the works mentioned above each laminate has been assumed to be isotropic. In this paper a stiffness method is presented for studying harmonic wave propagation in a periodically laminated medium, where each lamina may have anisotropic properties. For the purpose of clarity antiplane and plane strain motions are dealt with separately. An interpolation function is assumed for each lamina and is characterized by a discrete number of generalized coordinates at the interfaces. These generalized coordinates are the interface displacements and stresses, thus ensuring the continuity of stresses and displacements across the bounding planes. By applying Hamilton's principle and using Floquet's theory the dispersion equation is obtained as a standard algebraic eigenvalue problem whose solution yields the dispersion relations as well as the variation of stresses and the displacements. To assess the accuracy of this method the numerical results are first compared with the existing results[15, 17] for the isotropic case. It is shown that most of the important features of the surface in frequency-wave number space are reproduced. Numerical results are then presented for a boron fiber-reinforced aluminum composite. The attractiveness of the method presented is in the relative ease with which it can be used to study wave propagation in layered media with anisotropic layers. In the following equations are developed for this general case and then are specialized for the isotropic case.

EQUATIONS OF LINEAR ELASTICITY

We consider harmonic waves propagating through a two-layer periodically laminated elastic body of unbounded extent (Fig. 1). Any two adjacent laminates in the body then comprise a unit cell. Both laminates in the unit cell are assumed to be homogeneous, ortho-rhombic, and

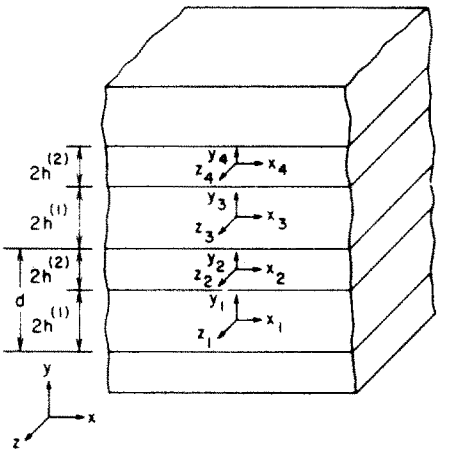

Fig. 1. Geometry of periodically laminated infinite elastic solid.

perfectly bonded to contiguous laminates. The stress-strain relation for each laminate in a cell is:

$$\begin{aligned}
\sigma_{xx}^{(i)} &= C_{11}^{(i)}E_{xx}^{(i)} + C_{12}^{(i)}E_{yy}^{(i)} + C_{13}^{(i)}E_{zz}^{(i)} \\
\sigma_{yy}^{(i)} &= C_{12}^{(i)}E_{xx}^{(i)} + C_{22}^{(i)}E_{yy}^{(i)} + C_{23}^{(i)}E_{zz}^{(i)} \\
\sigma_{zz}^{(i)} &= C_{13}^{(i)}E_{xx}^{(i)} + C_{23}^{(i)}E_{yy}^{(i)} + C_{33}^{(i)}E_{zz}^{(i)} \\
\sigma_{yz}^{(i)} &= C_{44}^{(i)}\gamma_{xy}^{(i)}, \qquad \sigma_{xz}^{(i)} = C_{55}^{(i)}\gamma_{xt}^{(i)}, \qquad \sigma_{xy}^{(i)} = C_{66}^{(i)}\gamma_{xy}^{(i)}. \qquad (i = 1, 2)
\end{aligned} \tag{1}$$

where $\sigma_{ij}^{(i)}$, $E_{ij}^{(i)}$, $\gamma_{ij}^{(i)}$, and $C_{ij}^{(i)}$ are stresses, strains and material constants of the ith laminate, respectively. Each laminate has thickness $2h^{(i)}$ and density $\rho^{(i)}$, respectively. The laminated elastic body B is the union of all these cells.

Let $u^{(i)}(x_i, y_i, z_i; t)$, $v^{(i)}(x_i, y_i, z_i; t)$ and $w^{(i)}(z_i, y_i, z_i; t)$ be the Cartesian components of the displacement vector in the x, y, and z-direction, respectively, for the ith laminate (see Fig. 1).

Antiplane strain

For antiplane motion, we have

$$\begin{aligned}
u^{(i)}(x_i, y_i, z_i; t) = 0; \qquad v^{(i)}(x_i, y_i, z_i; t) = 0; \\
w^{(i)}(x_i, y_i, z_i; t) = w^{(i)}(x_i, y_i; t).
\end{aligned} \tag{2}$$

Substituting eqn (2) into strain-displacement equations, and these, in turn, in eqn (1) we obtain stress-displacement relations. Substituting the stress-displacement relations into stress equations of motions, Navier equations of motion can be obtained. Solving the Navier equations we can evaluate the displacement and stress in each laminate.

Dispersion relation is obtained by applying the following interface stress and continuity conditions,

$$\begin{aligned}
w^{(2)}(x_2, -h^{(2)}; t) &= w^{(1)}(x_i, h^{(1)}; t) \\
\sigma_{yz}^{(2)}(x_2; -h^{(2)}; t) &= \sigma_{yz}^{(1)}(x_1, h^{(1)}; t)
\end{aligned} \tag{3a}$$

$$\begin{aligned}
w^{(2)}(x_2, h^{(2)}; t) &= w^{(3)}(x_3, -h^{(1)}; t) \\
\sigma_{yz}^{(2)}(x_2, h^{(2)}; t) &= \sigma_{yz}^{(3)}(x_3, -h^{(1)}; t).
\end{aligned} \tag{3b}$$

The quasi-periodicity of the Floquet solution[18] may be used to rewrite the two equations (3b) in the form

$$w^{(2)}(x_2, h^{(2)}; t) = w^{(1)}(x_1, -h^{(1)}; t)\, e^{ik_y d}$$

$$\sigma_{yz}^{(2)}(x_2, h^{(2)}; t) = \sigma_{yz}^{(1)}(x_1, -h^{(1)}; t)\, e^{ik_y d}, \tag{4}$$

where $i = \sqrt{-1}$, k_y is the Floquet wave number and $d = 2(h^{(1)} + h^{(2)})$.

For isotropic laminates, using eqns (3a) and (3b), Sun *et al.*[11], and Lee and Yang[12] obtained the dispersion equation for the wave propagating normal to the laminates, while Robinson[13] obrained the dispersion equation for the general case. Recently, Delph *et al.*[15] obtained the dispersion equation using eqns (3a) and (4). The equation, in general, is a 4×4 determinant whose elements are complex valued transcendental functions of frequency, wave numbers, and depend on the geometric and material properties.

Plane strain

For plane strain motion, we have

$$\begin{aligned} u^{(i)}(x_i, y_i, z_i; t) &= u^{(i)}(x_i, y_i; t) \\ v^{(i)}(x_i, y_i, z_i; t) &= v^{(i)}(x_i, y_i; t) \\ w^{(i)}(x_i, y_i, z_i; t) &= 0. \end{aligned} \tag{5}$$

By carrying out similar oerations as explained for the Antiplane Strain case the dispersion equation is obtained by applying the interface traction and displacement continuity equations as

$$\begin{aligned} u^{(2)}(x_2, -h^{(2)}; t) &= u^{(1)}(x_1, h^{(1)}; t) \\ v^{(2)}(x_2, -h^{(2)}; t) &= v^{(1)}(x_1, h^{(1)}; t) \\ \sigma_{xy}^{(2)}(x_2, -h^{(2)}; t) &= \sigma_{xy}^{(1)}(x_1, h^{(1)}; t) \\ \sigma_{yy}^{(2)}(x_2, -h^{(2)}; t) &= \sigma_{yy}^{(1)}(x_1, h^{(1)}; t) \end{aligned} \tag{6a}$$

and

$$\begin{aligned} u^{(2)}(x_2, h^{(2)}; t) &= u^{(3)}(x_3, -h^{(1)}; t) \\ v^{(2)}(x_2, h^{(2)}; t) &= v^{(3)}(x_3, -h^{(1)}; t) \\ \sigma_{xy}^{(2)}(x_2, h^{(2)}; t) &= \sigma_{xy}^{(3)}(x_3, -h^{(1)}, t) \\ \sigma_{yy}^{(2)}(x_2, h^{(2)}; t) &= \sigma_{yy}^{(3)}(x_3, -h^{(1)}, t). \end{aligned} \tag{6b}$$

Using Floquet's theory, the four equations (6b) can be rewritten in the form

$$\begin{aligned} u^{(2)}(x_2, h^{(2)}; t) &= u^{(1)}(x_1, -h^{(1)}; t)\, e^{ik_y d} \\ v^{(2)}(x_2, h^{(2)}; t) &= v^{(1)}(x_1, -h^{(1)}; t)\, e^{ik_y d} \\ \sigma_{xy}^{(2)}(x_2, h^{(2)}; t) &= \sigma_{xy}^{(1)}(x_1, -h^{(1)}; t)\, e^{ik_y d} \\ \sigma_{yy}^{(2)}(x_2, h^{(2)}; t) &= \sigma_{yy}^{(1)}(x_1, -h^{(1)}; t)\, e^{ik_y d}. \end{aligned} \tag{7}$$

For isotropic laminates, Sve[14] used eqns (6a, b) while Delph *et al.*[16, 17] used eqns (6a) and (7) to obtain the dispersion equation. The dispersion equation, in general, is an 8×8 determinant with elements that are transcendental functions.

In the following we present a general method of obtaining approximate dispersion equations by a stiffness method which is applicable to both isotropic and anisotropic laminates having m-layer periodicity. For the sake of simplicity the method is presented for antiplane and plane strain motions. However, it can easily be used for the three-dimensional case.

APPROXIMATE SOLUTION METHOD

Let us consider a periodically laminated elastic body of unbounded extent with unit cell consisting of m laminas as shown in Fig. 2. Thus, it is possible to model each laminate of Fig.

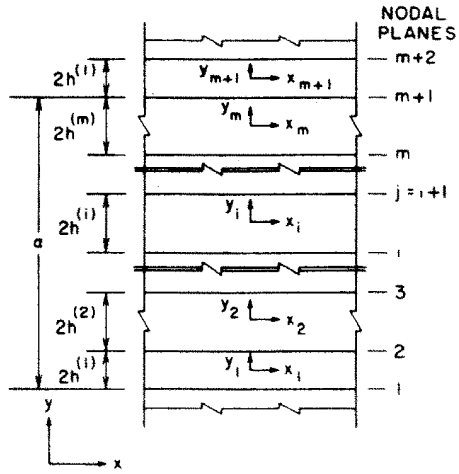

Fig. 2. m-layered periodicity.

1 with a number of laminas in order to achieve a better physical representation. Each lamina is assumed to be homogeneous, ortho-rhombic, and perfectly bonded to contiguous laminas. Laminar bounding planes are designated as nodal planes in Fig. 2.

Antiplane strain

For the antiplane motion the interpolation function for the ith lamina is taken to be of cubic form,

$$w^{(i)}(x_i, y_i; t) = \left\{ f_1(\eta_i) w_i + f_2(\eta_i) w_j + f_3(\eta_i) \frac{\beta_i}{c_{44}^{(i)}} + f_4(\eta_i) \frac{\beta_j}{c_{44}^{(i)}} \right\} e^{i(k_x x - \omega t)} \tag{8}$$

where k_x is the wave number in x direction, ω is the circular frequency, $j = i + 1$,

$$\begin{aligned} w_i &= w^{(i)}(x_i, -h^{(i)}); \qquad w_j = w^{(i)}(x_i, h^{(i)}) \\ \beta_i &= \sigma_{yz}^{(i)}(x_i, -h^{(i)}); \qquad \beta_j = \sigma_{yz}^{(i)}(x_i, h^{(i)}) \end{aligned} \tag{9}$$

w_i, β_i are complex-valued amplitudes of the ith nodal displacement and stress, respectively. The $f_m(\eta_i)$ appearing in eqn (8) are given by

$$\begin{aligned} f_1(\eta_i) &= (2 - 3\eta_i + \eta_i^3)/4 \\ f_2(\eta_i) &= (2 + 3\eta_i - \eta_i^3)/4 \\ f_3(\eta_i) &= (1 - \eta_i - \eta_i^2 + \eta_i^3) h^{(i)}/4 \\ f_4(\eta_i) &= (-1 - \eta_i + \eta_i^2 + \eta_i^3) h^{(i)}/4 \end{aligned} \tag{10}$$

where $\eta_i = y_i/h^{(i)}$.

Interpolation function (8) is so chosen as to satisfy interface stress and displacement continuity conditions (3a). The potential energy and kinetic energy for the ith lamina are obtained by integrating over both the lamina thickness and the wavelength L,

$$\begin{aligned} V_1^{(i)} &= \frac{1}{2} \int_0^L \int_{-h^{(i)}}^{h^{(i)}} [c_{44}^{(i)} \gamma_{yz}^{(i)} \bar{\gamma}_{yz}^{(i)} + c_{55}^{(i)} \gamma_{xz}^{(i)} \bar{\gamma}_{xz}^{(i)}] \, dx_i \, dy_i \\ T_1^{(i)} &= \frac{\omega^2}{2} \int_0^L \int_{-h^{(i)}}^{h^{(i)}} \rho^{(i)} w^{(i)} \bar{w}^{(i)} \, dx_i \, dy_i \end{aligned} \tag{11}$$

where bar over the quantity designates the complex-conjugate. After differentiating the assumed displacement field, its substitution into the potential and kinetic energy expressions

leads to forms given in the matrix notation by

$$V_1^{(i)} = \frac{1}{2}\{\bar{r}_1\}^T[k_1]\{r_1\}$$

$$T_1^{(i)} = \frac{1}{2}\{\bar{r}_1\}^T[m_1]\{r_1\} \tag{12}$$

where $\{r_1\}^T = \{w_i\beta_i w_j\beta_j\}^T$, and $[k_1]$ and $[m_1]$ are the stiffness and mass matrices of the lamina. Explicit form of $[s^a] = (1/L)[k_1 - \omega^2 m_1]$ is given in Appendix A. It may be noted that the matrix s^a is real.

By summing over all the laminas the Hamiltonian H_1 can be defined as

$$H_1 = \sum (V^{(i)} - T^{(i)}). \tag{13}$$

Floquet's solution (4) can be written in the form

$$\{w_{m+1}\beta_{m+1}w_{m+2}\beta_{m+2}\}^T = \{w_1\beta_1 w_2\beta_2\}^T e^{ik_y d} \tag{14}$$

where

$$d = \sum_{i=1}^{m} 2h^{(i)}.$$

Applying Hamilton's principle to (13) and then utilizing the Floquet's relation (14), we can write the equilibrium equations for nodes 2 to $m+1$. After rearranging terms, these equations yield the dispersion relation as an algebraic eigenvalue problem

$$[A_1]\{R_1\} = \omega^2[B_1]\{R_1\}, \tag{15}$$

where $\{R_1\}^T = \{w_1\beta_1 w_2\beta_2 \ldots w_m\beta_m\}$, and $[A_1]$ and $[B_1]$ are $2m \times 2m$ complex-valued matrices, whose elements depend on the material and geometric properties and are polynomial functions of the wave numbers k_x and k_y.

Plane strain

Steps followed in deriving the dispersion relation for plane strain motion are the same as those used in the antiplane strain case. Interpolation functions satisfying interface stress and displacement continuity conditions (6a) are assumed to be of the forms

$$\begin{Bmatrix} u^{(i)} \\ v^{(i)} \end{Bmatrix} = e^{i(k_x x - \omega t)} \begin{bmatrix} u_i u_j & \dfrac{\tau_i}{c_{66}^{(i)}} - \dfrac{\partial v_i}{\partial x_i} & \dfrac{\tau_i}{c_{66}^{(i)}} - \dfrac{\partial v_j}{\partial x_i} & \\ v_i v_j & \dfrac{\sigma_i}{c_{22}^{(i)}} - \dfrac{c_{12}^{(i)}}{c_{22}^{(i)}} \dfrac{\partial u_i}{\partial x_i} & \dfrac{\sigma_j}{c_{22}^{(i)}} - \dfrac{c_{12}^{(i)}}{c_{22}^{(i)}} & \dfrac{\partial u_j}{\partial x_i} \end{bmatrix} \begin{Bmatrix} f_1(\eta_i) \\ f_2(\eta_i) \\ f_3(\eta_i) \\ f_4(\eta_i) \end{Bmatrix} \tag{16}$$

where $j = i + 1$,

$$\{u_i\tau_i v_i\sigma_i\}^T = \{u^{(i)}\sigma_{xy}^{(i)}v^{(i)}\sigma_{yy}^{(i)}\}^T_{y_i = -h^{(i)}}$$

$$\{u_j\tau_j v_j\sigma_j\}^T = \{u^{(i)}\sigma_{xy}^{(i)}v^{(i)}\sigma_{yy}^{(i)}\}^T_{y_i = h^{(i)}}$$

and $f_m(\eta_i)$ are given by eqn (10). For brevity of presentation the case of real k_x is presented here.

The potential energy and kinetic energy for the ith lamina are

$$V_2^{(i)} = \frac{1}{2}\int_0^L \int_{-h^{(i)}}^{h^{(i)}} (\sigma_{xx}\bar{\varepsilon}_{xx}^{(i)} + \sigma_{yy}^{(i)}\bar{\varepsilon}_{yy}^{(i)} + \sigma_{xy}\bar{\gamma}_{xy}^{(i)})\, dx_i\, dy_i$$

$$T_2^{(i)} = \frac{\omega^2}{2}\int_0^L \int_{-h^{(i)}}^{h^{(i)}} \rho^{(i)}(u^{(i)}\bar{u}^{(i)} + v^{(i)}\bar{v}^{(i)})\, dx_i\, dy_i. \tag{17}$$

After differentiating the assumed displacement fields (16), substituting them into energy expressions, integrating over one wavelength L, leads to

$$V_2^{(i)} = \frac{1}{2}\{\bar{r}_2\}^T[k_2]\{r_2\},$$
$$T_2^{(i)} = \frac{1}{2}\{\bar{r}_2\}^T[m_2]\{r_2\}, \tag{18}$$

where $\{r_2\}^T = \{u_i\tau_i v_i\sigma_i u_j\tau_j v_j\sigma_j\}^T$, and $[k_2]$ and $[m_2]$ are the stiffness and mass matrices of the lamina. Explicit form of the Hermitian matrix $[s^p] = (1/L)[k_2 - \omega^2 m_2]$ is given in Appendix B.

Floquet's relation (7) can be written as

$$\{u_{m+1}\tau_{m+1}v_{m+1}\sigma_{m+1}u_{m+2}\tau_{m+2}v_{m+2}\sigma_{m+2}\}^T = \{u_1\tau_1 v_1\sigma_1 u_2\tau_2 v_2\sigma_2\}^T e^{ik_y d}. \tag{19}$$

Applying Hamilton's principle to (18) and using eqn (19) the equilibrium equations for nodes 2 to $m+1$ can be written. This yields the dispersion relations as an algebraic eigenvalue problem:

$$[A_2]\{R_2\} = \omega^2[B_2]\{R_2\}, \tag{20}$$

where $\{R_2\}^T = \{u_1\tau_1 v_1\sigma_1 \ldots u_m\tau_m v_m\sigma_m\}$, and $[A_2]$ and $[B_2]$ are $4m \times 4m$ complex-valued matrices with polynomial elements.

It may be mentioned that a stiffness analysis was employed by Dong and Nelson[19] in studying the vibration characteristic of laminated orthotropic plates. They employed an interpolation function satisfying only interface displacement continuity conditions.

Numerical results and discussion

For given material and geometric parameters, each of the dispersion eqns (15) and (20) relates frequency to two wave numbers. The roots of this equation define a surface in frequency-wave number space, which is the dispersion surface. This surface is in general discontinuous at $k_y = (n\pi/d)$, $n = 1, 2, \ldots$. These planes of discontinuity divide the surface into Brillouin zones. Each equation admits complex as well as real wave number k_y. At the end of the Brillouin zones, except $k_x = 0$, we get complex branches. Thus the surface can be interpreted in terms of passing and stopping bands. Also at the end of the Brillouin zones, we get symmetric-symmetric, antisymmetric-symmetric, and symmetric-antisymmetric variations of the displacement. When $k_x = 0$, the dispersion eqn (20) yields two $(2m \times 2m)$ equations. One of these equations is the dispersion equation for longitudinal (P) waves propagating normal to the laminates, while the other is for shear (S) waves propagating normal to the laminates.

To guage the accuracy and range of applicability of this approach, we consider in Example 1 a two-layered periodic isotropic laminated medium. The numerical results, from elasticity solutions for this case, are presented by Delph *et al.*[15, 17]. In Example 2, we consider a particular case of a boron fiber-reinforced aluminum composite[20].

Example 1. *Isotopic laminates.* The material and geometric properties of this two-layered periodic composite are

$$\epsilon = h^{(1)}/h^{(2)} = 4, \qquad \gamma = c_{66}^{(2)}/c_{66}^{(1)} = 0.02, \qquad \sigma^2 = \frac{c_{66}^{(2)}\rho^{(1)}}{c_{66}^{(1)}\rho^{(2)}} = 0.06.$$

The Poisson's ratios are $\nu^{(1)} = 0.35$ and $\nu^{(2)} = 0.3$.

Each laminate was subdivided into two and then three laminas, thus creating four- and six-layered periodicity. It was noticed that the results for lower modes did not appreciably change by increasing the number of laminas. Results of four-layered periodicity are presented here. Most of the figures of [15, 17] were reproduced by our method, only a few are given here for illustration purposes.

In Figs. 3–6 we present our results for antiplane motion while in Figs. 7–10 we present the

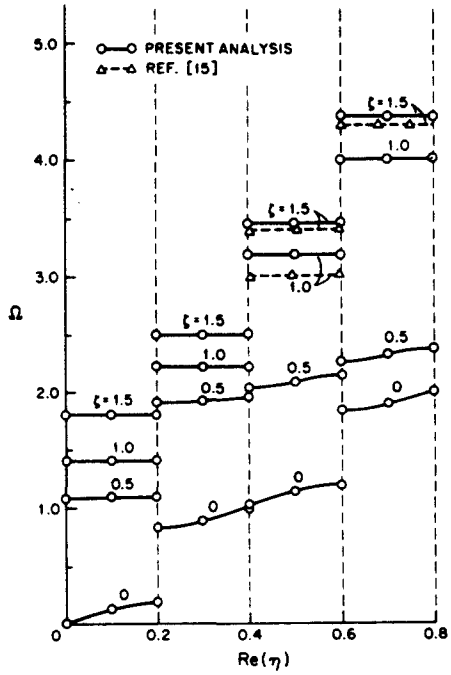

Fig. 3. Curves of constant ζ on the antiplane-strain dispersion surface.

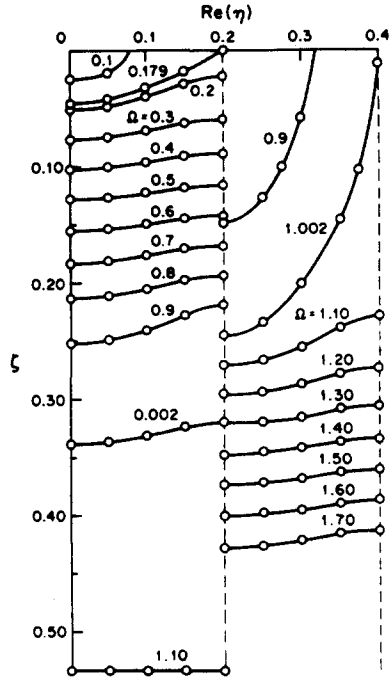

Fig. 4. Curves of constant Ω on the antiplane-strain dispersion surface.

results for plane strain motion. Wherever there is deviation we have plotted results from Refs. [15, 17].

The results are presented in non-dimensional form as

$$\eta = \frac{2h^{(2)}k_y}{\pi}, \qquad \zeta = \frac{2h^{(2)}k_x}{\pi}, \qquad \Omega = \frac{2h^{(2)}\omega}{\pi}\sqrt{\left(\frac{\rho^{(2)}}{c_{66}^{(2)}}\right)}. \tag{21}$$

Figure 3 shows some results for the first four Brillouin zones for sections of the surface

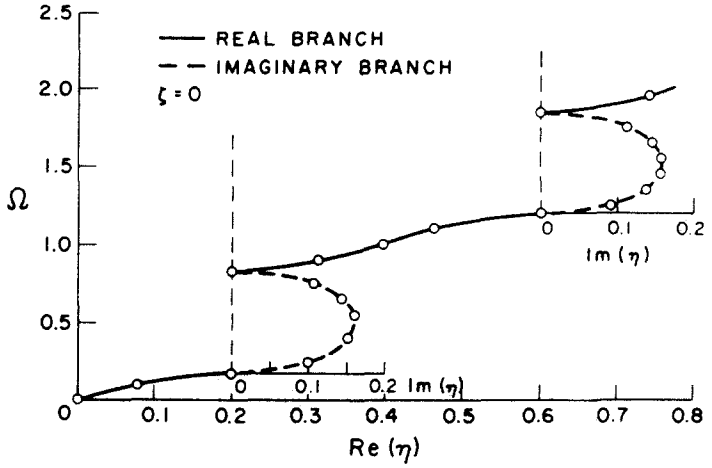

Fig. 5. Antiplane-strain dispersion surface in the $\zeta = 0$ plane with complex branches.

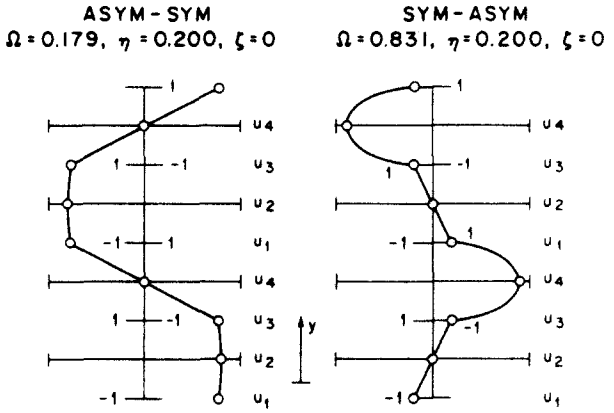

Fig. 6. Mode shapes at points on the ends of Brillouin zones ($\zeta = 0$).

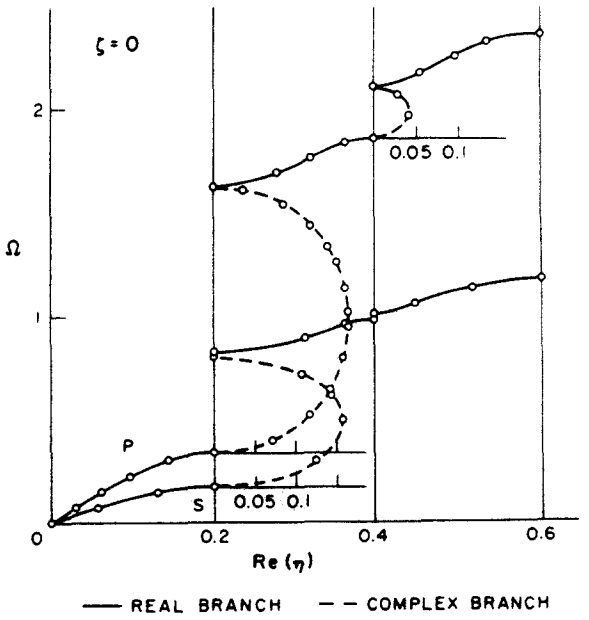

Fig. 7. P and S surfaces in $\zeta = 0$ plane with complex branches.

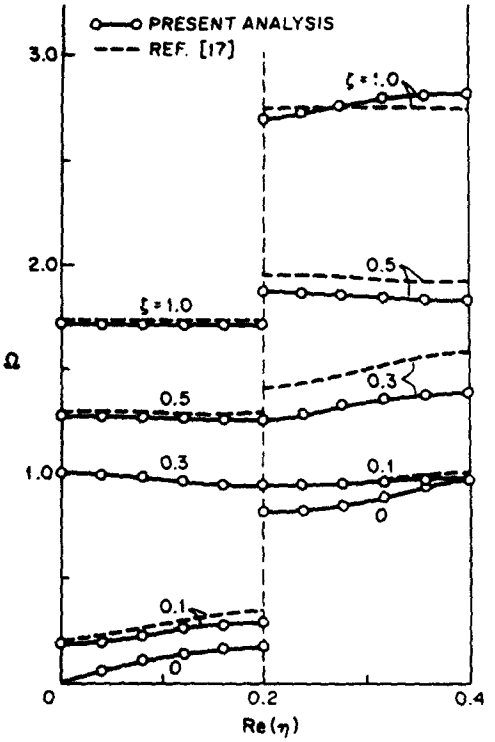

Fig. 8. Curves of constant ζ on the S-surface.

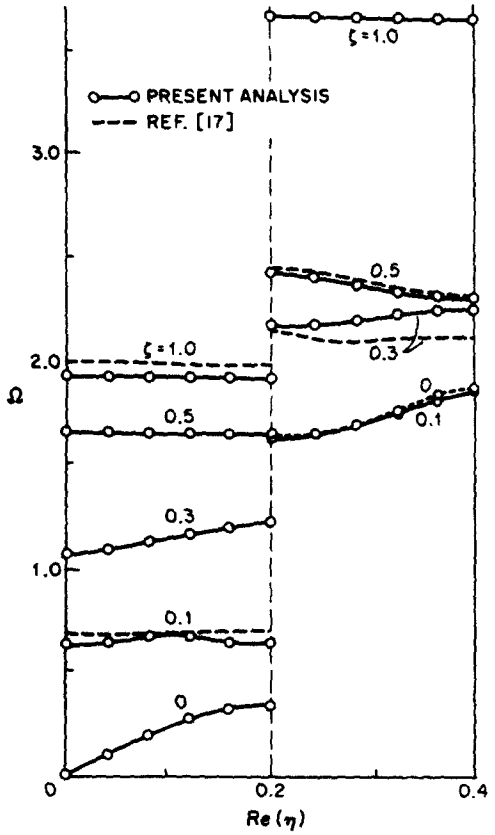

Fig. 9. Curves of constant ζ on the P-surface.

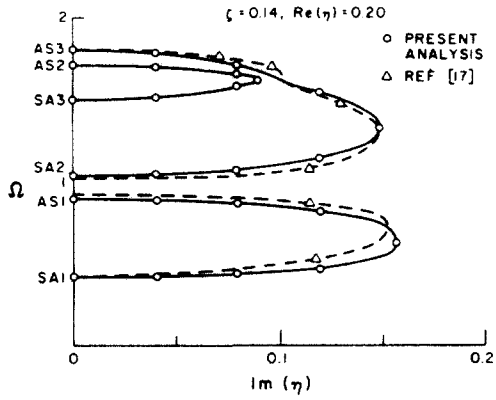

Fig. 10. Complex branches for Re $(\eta) = 0.2$, $\zeta = 0.14$.

lying in planes of constant ζ, while Fig. 4 shows curves of constant frequency on the surface for the first two Brillouin zones. Figure 5 shows both the real and complex branches for a protion of the surface in $\zeta = 0$ plane. Here the imaginary η-axis has been plotted on the real plane for clarity. Along the complex branches, the real part of η remains constant while the imaginary part varies. Figure 6 shows the mode shapes at $\zeta = 0$ for the first antisymmetric–symmetric and symmetric–antisymmetric branches. In general matching with the results of [15] is excellent for all ranges of ζ and η.

The dispersion curves for P and S waves propagating normal to the layering are sketched on an extended zone scheme in Fig. 7 over the first three Brillouin zones. The complex branches originating at the ends of the Brillouin zones are also included, where the imaginary axis has been rotated onto the real plane for clarity. Figure 8 shows the intersection of the S surface with planes of constant ζ over the first two Brillouin zones, while Fig. 9 shows the intersection of the P surface with planes of constant ζ over the two Brillouin zones. Figure 10 shows the complex branches for Re $(\eta) = 0.2$ and $\zeta = 0.14$. In this case of plane strain, it was found that good results were obtained for $\zeta < 1$. Increasing the number of laminas did not appreciably improve the results.

Example 2. Fiber-reinforced boron–aluminum composite. The method outlined earlier is now used to derive the dispersion characteristics in a fiber-reinforced composite. The example chosen is that of boron-fiber reinforced layers sandwiched between thin layers of aluminum. The material and geometric parameters are chosen as [20],

$$c_{11}^{(1)} = 2.45, \quad c_{12}^{(1)} = 0.604, \quad c_{22}^{(1)} = 1.7970, \quad c_{66}^{(1)} = 0.566$$

$$c_{11}^{(2)} = c_{22}^{(2)} = 1.017, \quad c_{12}^{(2)} = 0.573, \quad c_{66}^{(2)} = 0.267$$

$$\rho^{(1)} = 2.534\ \text{g/cm}^3, \quad \rho^{(2)} = 2.702\ \text{g/cm}^3, \quad \epsilon = \frac{h^{(1)}}{h^{(2)}} = 9.$$

The units for c_{ij} are 10^{11} N/m^2. Here the superscript (1) refers to the fiber-reinforced layer and (2) refers to the aluminum layer. The x-axis is taken parallel to the fiber direction.

Figures 11–13 show the dispersion curves. The dispersion curves for the P- and S-waves are sketched on an extended zone scheme in Fig. 11 over the first two Brillouin zones. The complex branches originating at the ends of the Brillouin zones are sketched also. It is noted that since the material properties of the two layers are not markedly different visible complex branch does not start until the third mode. Figures 12 and 13 show the intersections of the quasi-shear and quasi-longitudinal wave surfaces with planes of constant ζ over the first two Brillouin zones. The marked departure in the behavior of the $\zeta \neq 0$ branches from the $\zeta = 0$ branch is quite significant.

CONCLUSION

It has been shown that the stiffness method presented here using the continuity of displacements and tractions and the Floquet's theory gives excellent results for the lower

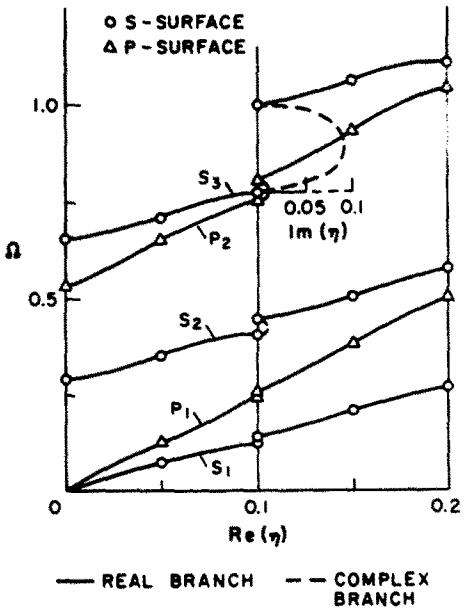

Fig. 11. P and S surfaces in $\zeta = 0$ plane with complex branches for fiber-reinforced medium.

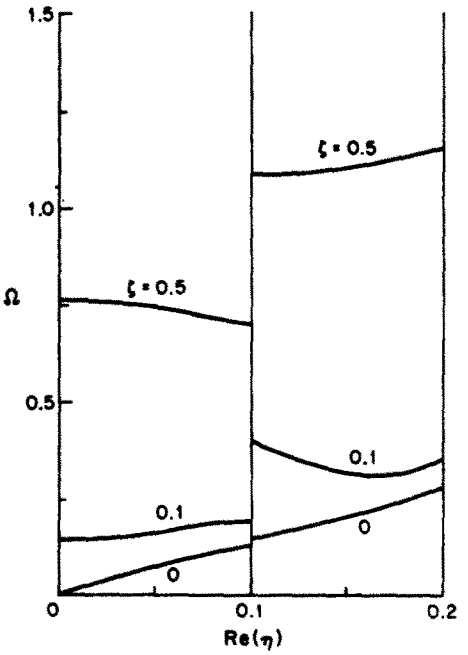

Fig. 12. Curves of constant ζ on S-surface for fiber-reinforced medium.

modes of wave propagation in a layered composite. Even at higher modes the results are in good agreement with the available exact solutions for isotropic layers. As indicated before, one major advantage of the method is that the determinantal equation governing dispersion involves only polynomial functions of the wave number and the frequency, whereas these are transcendental in the exact solution. Another advantage of this technique is its applicability to two- and three-dimensional problems of wave propagation in anisotropic layers. In this paper only the two-dimensional problem has been studied. The solution to the three-dimensional problem will be presented in a future communication.

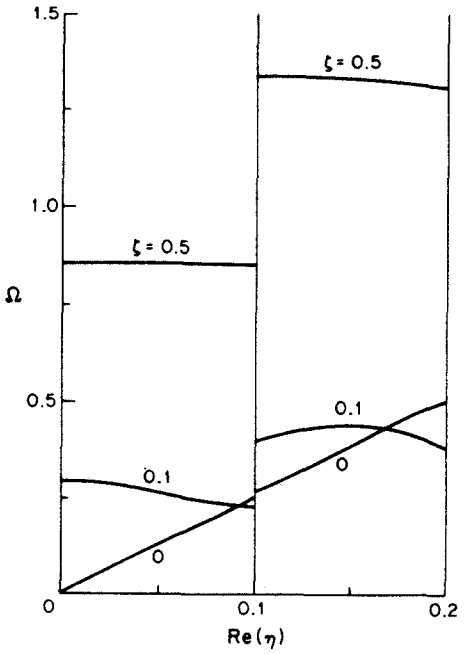

Fig. 13. Curves of constant ζ on P-surface for fiber-reinforced medium.

Acknowledgements—This work has been supported in part by a grant CME 78-24179 from the National Science Foundation and a grant A-7988 from the Natural Science and Engineering Council of Canada. The authors are also grateful to Mr. Roy Swanson and Mr. Patrick Lo for help in the numerical computations.

REFERENCES

1. G. W. Postma, Wave propagation in a stratified medium. *Geophysics* **20**, 780 (1955).
2. S. M. Rytov, The acoustical properties of a thinly laminated medium. *Soviet Phys. Acoustics* **2**, 67 (1956).
3. C. T. Sun, J. D. Achenbach and G. Herrmann, Continuum theory for a laminated medium. *J. Appl. Mech.* **35**, 467 (1968).
4. J. D. Achenbach, Generalized continuum theories for directionally reinforced solids. *Archiv. Mech.* **28**, 257 (1976).
5. A. Bedford and M. Stern, Toward a diffusing continuum theory of composite materials. *J. Appl. Mech.* **38**, 8 (1971).
6. A. Bedford and M. Stern, A multicontinuum theory of composite materials. *Acta Mechanica* **14**, 85 (1972).
7. H. D. McNiven and Y. Mengi, A mixture theory for elastic laminated composites. *Int. J. Solids Structures* **15**, 281 (1979).
8. G. A. Hegemier, On a theory of interacting continua for wave propagation in composites. *Dynamics of Composite Materials*, p. 70. The American Society of Mechanical Engineers (1972).
9. G. A. Hegemier and T. C. Bache, A general continuum theory with microstructure for wave propagation in elastic laminated composites. *J. Appl. Mech.* **41**, 101 (1974).
10. Y. Mengi, G. Birlik and H. D. McNiven, A new approach for developing dynamic theories for structural elements—2. Application to thermoelastic layered composites. *Int. J. Solids Structures* **16**, 1169 (1980).
11. C. T. Sun, J. D. Achenbach and G. Herrmann, Time-harmonic waves in a stratified medium propagating in the direction of the layering. *J. Appl. Mech.* **35**, 408 (1968).
12. E. H. Lee and W. H. Yang, On waves in composite materials with periodic structures. *SIAM J. Appl. Math.* **25**, 492 (1973).
13. C. W. Robinson, *Shear Waves in Layered Composites*. Sandia Laboratories, Livermore, California (1972).
14. C. Sve, Time-harmonic waves travelling obliquely in a periodically laminated medium. *J. Appl. Mech.* **38**, 477 (1971).
15. T. J. Delph, G. Herrmann and R. K. Kaul, Harmonic waves propagation in a periodically layered, infinite elastic body: antiplane strain. *J. Appl. Mech.* **45**, 343 (1978).
16. T. J. Delph, G. Herrmann and R. K. Kaul, Harmonic wave propagation in a periodically layered, infinite elastic body: plane strain, analytical results. *J. Appl. Mech.* **46**, 113 (1979).
17. T. J. Delph, G. Herrmann and R. K. Kaul, Harmonic wave propagation in periodically layered, infinite elastic body: plane strain, numerical results. *J. Appl. Mech.* **47**, 531 (1980).
18. E. I. Ince, *Ordinary Differential Equations*. Dover Publications, New York (1956).
19. S. B. Dong and R. B. Nelson, On natural vibrations and waves in laminated orthotropic plates. *J. Appl. Mech.* **39**, 739 (1972).
20. S. K. Datta and H. M. Ledbetter, Anisotropic elastic constants of a fiber-reinforced boron–aluminum composite. In: *Mechanics of Nondestructive Testing* (Edited by W. W. Stinchcomb). Plenum Press, New York (1980).

APPENDIX A

Elements of $[s^a]$ *matrix for antiplane strain*

Omitting the superscript i for the ith lamina and defining

$$Q = (c_{55}k_x^2 - \omega^2), \tag{A1}$$

the elements of the symmetric $[s^a]$ matrix are given by

$$
\begin{aligned}
s^a_{11} &= s^a_{33} = \frac{3}{5}\frac{c_{44}}{h} + \frac{78h}{105}Q,\\
s^a_{12} &= -s^a_{34} = \frac{1}{10} + \frac{22h^2}{105c_{44}}Q,\\
s^a_{13} &= -\frac{3}{5}\frac{c_{44}}{h} + \frac{9h}{35}Q,\\
s^a_{14} &= -s^a_{23} = \frac{1}{10} - \frac{13h^2}{105c_{44}}Q,\\
s^a_{22} &= s^a_{44} = \frac{4h}{15c_{44}} + \frac{8h^3}{105c^2_{44}}Q,\\
s^a_{24} &= -\frac{h}{15c_{44}} - \frac{6h^3}{105c^2_{44}}Q.
\end{aligned}
\tag{A2}
$$

APPENDIX B

Elements of $[s^p]$ *matrix for plane strain*

Omitting the superscript i for the ith lamina and defining

$$
\begin{aligned}
Q_1 &= h(c_{11}k_x^2 - \omega^2), \qquad Q_2 = h(c_{66}k_x^2 - \omega^2),\\
Q_3 &= k_x(c_{12} + c_{66}); \qquad Q_4 = c_{12}/c_{22},
\end{aligned}
\tag{B1}
$$

the elements of the Hermitian matrix $[s^p]$ are given by

$$
\begin{aligned}
s^p_{11} &= s^p_{55} = \frac{78}{105}Q_1 + \frac{3}{5}\frac{c_{66}}{h} + \frac{8h^2}{105}k_x^2Q_4^2c_{22} + \frac{4h}{15}k_x^2Q_4^2c_{22} - \frac{2}{5}hk_xQ_4Q_3,\\
s^p_{12} &= -s^p_{56} = \frac{22h}{105c_{66}}Q_1 + \frac{1}{10},\\
s^p_{13} &= -s^p_{57} = i\left\{-\frac{22h}{105}k_xQ_1 - \frac{k_xc_{66}}{10} + \frac{22h}{105}k_xQ_4Q_2\right.\\
&\qquad \left. + \frac{k_xQ_4}{10}c_{22} + \frac{k_x}{2}(c_{12} - c_{66})\right\},\\
s^p_{14} &= s^p_{58} = -\frac{ihQ_3}{5c_{22}},\\
s^p_{15} &= \frac{9}{35}Q_1 - \frac{3c_{66}}{5h} - \frac{6h^2}{105}k_x^2Q_4^2Q_2 - \frac{h}{15}k_x^2Q_4^2c_{22} + \frac{2h}{5}k_xQ_4Q_3,\\
s^p_{16} &= -\frac{13h}{105c_{66}}Q_1 + \frac{1}{10} - \frac{h^2k_xQ_4Q_3}{15c_{66}},\\
s^p_{17} &= i\left\{\frac{13h}{c_{66}}k_xQ_1 - \frac{k_x}{10}c_{66} + \frac{13h}{105}k_xQ_4Q_2 - \frac{k_xQ_4}{10}c_{22} + \left(\frac{1}{2} - \frac{h^2}{15}k_x^2Q_4\right)Q_3\right\},\\
s^p_{18} &= i\left\{-\frac{6h^2k_x}{105c_{22}}Q_4Q_2 - \frac{hk_xQ_4}{15} + \frac{hQ_3}{5c_{22}}\right\},\\
s^p_{22} &= s^p_{66} = \frac{8h^2}{105c^2_{66}}Q_1 + \frac{4h}{15c_{66}},\\
s^p_{23} &= s^p_{67} = \frac{ihQ_3}{5c_{66}}; \qquad s^p_{24} = s^p_{68} = 0,\\
s^p_{25} &= \frac{13hQ_1}{105c_{66}} - \frac{1}{10} + \frac{h^2k_x}{15c_{66}}Q_4Q_3,\\
s^p_{26} &= -\frac{6h^2Q_1}{105c^2_{66}} - \frac{h}{15},\\
s^p_{27} &= i\left\{\frac{6h^2k_xQ_1}{105c_{66}} + \frac{hk_x}{15} - \frac{hQ_3}{5c_{66}}\right\},\\
s^p_{28} &= ih^2Q_3/15c_{22}c_{66},\\
s^p_{33} &= s^p_{77} = \frac{8h^2}{15}k_x^2Q_1 + \frac{4h}{15}k_x^2c_{44} + \frac{78}{105}Q_2 + \frac{3c_{22}}{5h} - \frac{2hk_xQ_3}{5},\\
s^p_{34} &= -s^p_{78} = \frac{22hQ_2}{105c_{22}} + \frac{1}{10},\\
s^p_{35} &= i\left\{\frac{13h}{105}k_xQ_1 - \frac{k_x}{10}c_{44} + \frac{13h}{105}k_xQ_4Q_2 - \frac{k_x}{10}c_{22}Q_4 - \left(\frac{1}{2} - \frac{h^2}{15}k_x^2Q_4\right)Q_3\right\},
\end{aligned}
$$

$$s_{36}^{P} = i\left\{\frac{6h^2k_xQ_1}{105c_{66}} - \frac{k_xh}{15} + \frac{hQ_3}{5c_{66}}\right\},$$

$$s_{37}^{P} = -\frac{6h^2k_x^2Q_1}{105} - \frac{hk_x^2c_{66}}{15} + \frac{9}{35}Q_2 - \frac{3}{5h}c_{22} + \frac{2hk_x}{5}Q_3$$

$$s_{38}^{P} = -\frac{13hQ_2}{105c_{22}} + \frac{1}{10} - \frac{h^2k_x}{15c_{22}}Q_3,$$

$$s_{44}^{P} = s_{88}^{P} = \frac{8h^2Q_2}{105c_{22}^2} + \frac{4h}{15c_{22}},$$

$$s_{45}^{P} = i\left\{\frac{6h^2k_x}{105c_{22}}Q_4Q_2 + \frac{hk_x}{15}Q_4 - \frac{hQ_3}{5c_{22}}\right\},$$

$$s_{46}^{P} = \frac{ih^2Q_3}{15c_{22}c_{66}},$$

$$s_{47}^{P} = \frac{13hQ_2}{105c_{22}} - \frac{1}{10} + \frac{h^2k_x}{15c_{22}}Q_3,$$

$$s_{48}^{P} = -\frac{6h^2Q_2}{105c_{22}^2} - \frac{h}{15c_{22}}. \tag{B2}$$